Available online at www.sciencedirect.com

ScienceDirect

Ciência & Tecnologia dos Materiais 27 (2015) 1–9

Ciência & Tecnologia dos MATERIAIS

http://ees.elsevier.com/ctmat

Special Issue PCF2014

J resistance curve behaviour of S355NL structural steel using the unloading compliance technique

Miguel A. V. de Figueiredo[a,*], Paulo M. S. T. de Castro[a]

[a] *Faculdade de Engenharia da Universidade do Porto, Rua Dr. Roberto Frias, 4200-465 Porto, Portugal*

Abstract

Room temperature toughness measurements performed on 32mm thick flat surface and side grooved C(T) specimens of the S355NL structural steel are presented. As expected, stable ductile crack growth was observed during the tests and toughness characterization based on resistance curve (R curve) concepts was therefore used. The unloading compliance technique was chosen to estimate stable crack growth during the tests, and accurate load line displacement measurements were performed using a clip gage. Stress intensity factor and compliance calibrations as a function of crack length/width ratio, published by ASTM, were used to derive the *J R*-curve. The *R*-curve for the flat surface specimen is higher than for the grooved specimen. The estimated *J* at initiation of stable crack propagation is also higher for the flat surface specimen, although difference between the flat and grooved specimens is very small. Generally, a drop in fracture toughness was observed for the grooved specimens, as expected given its higher triaxiality. As an additional comparison of the two types of specimens, the maximum load $J_{0,max}$ value was obtained using the actuator displacement record. The maximum load measurements proved to be rather similar in both types of specimen.

Keywords: Elasto-plastic fracture; Experimental Techniques; Resistance curve; Triaxiality.

1. Introduction

The interest for the unloading compliance technique for *J R*-curve characterization exists since the seventies of the last century; these were the early days of the development of Elastic Plastic Fracture Mechanics, under the main motivation of the safety of nuclear power plant, with initial contributions by Begley, Landes and others, *eg* [1-6]. This type of problems, together with interest for other forms of resistance curve behaviour, including applications in aeronautics using Al alloys, led to the development of the first standards for resistance curve (*R* curve) measurement, ASTM E561 [7].

The first standards for fracture toughness measurement concerned situations where Linear Elastic Fracture mechanics - LEFM could be applied, particularly the plane strain fracture toughness standard ASTM E399 [8]. Later, standards for elastic-plastic fracture were developed, as ASTM E813 or E1737, [9,10]. More recently, integrated standards covering a wide range of situations appeared, as ASTM E1820, [11] or BS7448, [12]. Basically the test consists in monotonically loading a pre-cracked specimen, characterizing the crack unstable or stable crack propagation through a variety of concepts, including critical stress intensity factor (*K*) or *J* integral and, in the case of stable crack propagation, resistance curves (*R*-curves). In this context reference should be made to the GKSS document 'EFAM GTP 02 - the GKSS test procedure for determining the fracture behaviour of materials' [13], that discusses in detail the several possible situations and alternatives, providing useful testing guidelines, and the ASTM

* Corresponding author.
E-mail address: mfiguei@fe.up.pt

http://dx.doi.org/10.1016/j.ctmat.2015.04.002

publication [14] reviewing the progress in this type of testing.

R-curves may of course be characterized using multiple specimens, each one of them loaded up to different maximum load level so that a range of crack extension values may be recorded. The unloading compliance technique is a less costly and less time consuming alternative to these tests. Usually it requires dedicated software that may automatically perform the partial unloadings at regular steps during testing, and eventually process all the data. In the present case, a standard servo-hydraulic machine, without dedicated software, was used in order to characterize the material behaviour.

The equations presented in ASTM E1820 [11] for (i) stress intensity factor (K) as a function of the crack length/width ratio (a/W), (ii) the relationship between a/W and compliance (C), and the determination of the effective value of thickness B_e in the case of grooved specimens, and (iii) the calculation of J_i as a function of K_i and of J_{pl} were used and are presented below.

For K,

$$K_i = \frac{P_i}{\sqrt{BB_N W}} f\left(\frac{a_i}{W}\right) \quad (1)$$

with:

$$f\left(\frac{a_i}{W}\right) = \frac{\left(2+\frac{a_i}{W}\right)}{\left(1-\frac{a_i}{W}\right)^{\frac{3}{2}}} \cdot X \quad (2)$$

$$X = 0.886 + 4.64\left(\frac{a_i}{W}\right) - 13.22\left(\frac{a_i}{W}\right)^2 + 14.72\left(\frac{a_i}{W}\right)^3 - 5.6\left(\frac{a_i}{W}\right)^4 \quad (3)$$

For the compliance,

$$\frac{a_i}{W} = 1.000196 - 4.06319u + 11.242u^2 - 106.043u^3 + 464.335u^4 - 650.677u^5 \quad (4)$$

with:

$$u = \frac{1}{\left[B_e E C_{c(i)}\right]^{\frac{1}{2}} + 1} \quad (5)$$

$$B_e = B - \frac{\left(B - B_N\right)^2}{B} \quad (6)$$

And for J calculation,

$$J_i = \frac{K_i^2\left(1-\nu^2\right)}{E} + J_{pl(i)} \quad (7)$$

with:

$$J_{pl(i)} = \frac{\eta_i A_{pl(i)}}{B_N\left(W - a_i\right)} \quad (8)$$

$$\eta_i = 2 + 0.522\left(1 - \frac{a_i}{W}\right) \quad (9)$$

2. Material and Specimens

Tables 1 and 2 present the chemical composition and basic mechanical data of the steel considered, S355NLZ15, already included in earlier papers on the fatigue crack growth behaviour of this steel [15,16], and Figure 1 presents details of the geometry of the specimens tested.

Table 1. Basic mechanical properties of the S355NLZ15 steel

Yield stress [Nmm^{-2}]	Rupture stress [Nmm^{-2}]	Elongation [%]	Charpy [J] at -50°C
400	557	27.7	176
405	516	30.2	118

Table 2. Chemical composition of the S355NLZ15 steel (weight %), 2 samples

C	Si	Mn	P	S	Al	N
0.14	0.28	1.23	0.013	0.004	0.027	0.007
0.13	0.24	1.11	0.011	0.005	0.022	0.007

Cr	Cu	Ni	Ti	V	Nb
0.008	0.31	0.29	0.016	0.044	0.001
0.006	0.25	0.27	0.013	0.043	0.001

One 20% deep 90° side-grooved specimen and one flat surface specimen, both with 32mm overall thickness, were tested for fracture toughness determination. The choice of 90°, corresponding to the upper limit of the possible range, [13], was due to availability of milling tool.

The knife edges used were 2mm thick, ensuring load line displacement measurement.

3. Tests and Data Treatment

Unloading compliance tests were performed at room temperature under quasi-static loading. Usually the unloading compliance technique requires dedicated software that may automatically perform the partial unloadings at regular steps during testing, and eventually process all the data. Here, a standard MTS servo-hydraulic machine without dedicated software was used to characterize the material *R*-curve behaviour.

Figure 2 gives the overall load versus clip gage displacement for the flat surface (a) and grooved specimen (b). A detail of the load versus clip gage for the initial elastic loading of each specimen is presented in Figure 3.For the sake of exemplification, Figure 4 shows the unloading compliance for one of the unloading steps performed in the flat surface specimen, revealing a typical plot of straight line and regular set of individual data points.

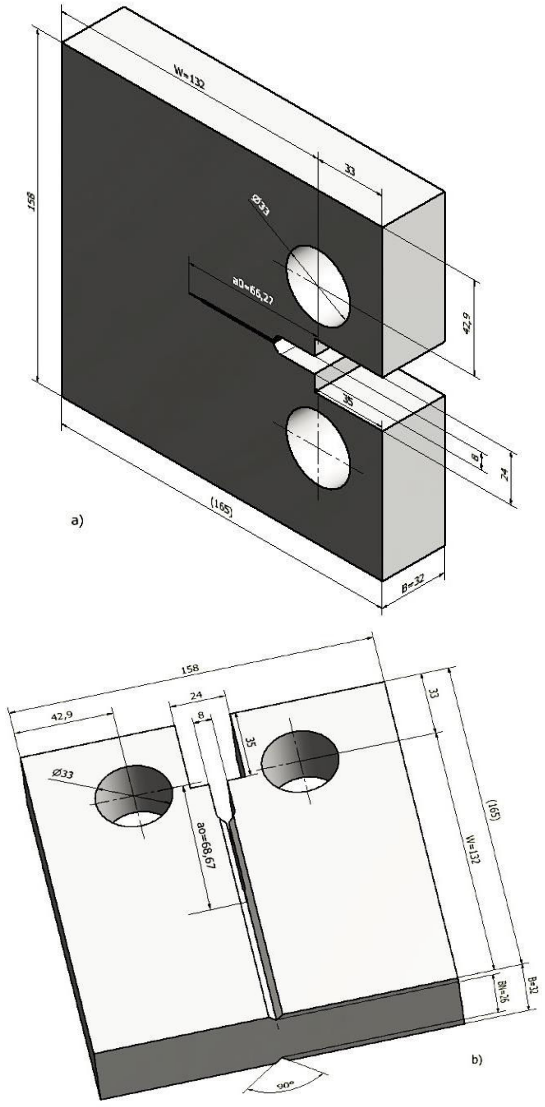

Fig. 1. a) Flat surface 32mm thick C(T) specimen; b) grooved C(T) specimen, with 20% side grooves in the crack plane.

Figure 5 is the compliance calibration $C = f(a/W)$ for the flat surface specimen, where using a_0 and C_0 as measured in the test, a Young's modulus of 205.36 GPa was inferred. This E value is very close to the expected value 210 GPa, the difference being only approximately 2.2%.

Figure 6 shows, for both specimens, the calculation of the relevant areas for performing the evaluation of J for each data point of the test (*ie*, for each unloading performed). For each unloading point on the load displacement-curve, 'area' means the integral of the curve up to that point, whereas 'corrected area' means the previous value less the elastic triangular area shown in Figure 6.

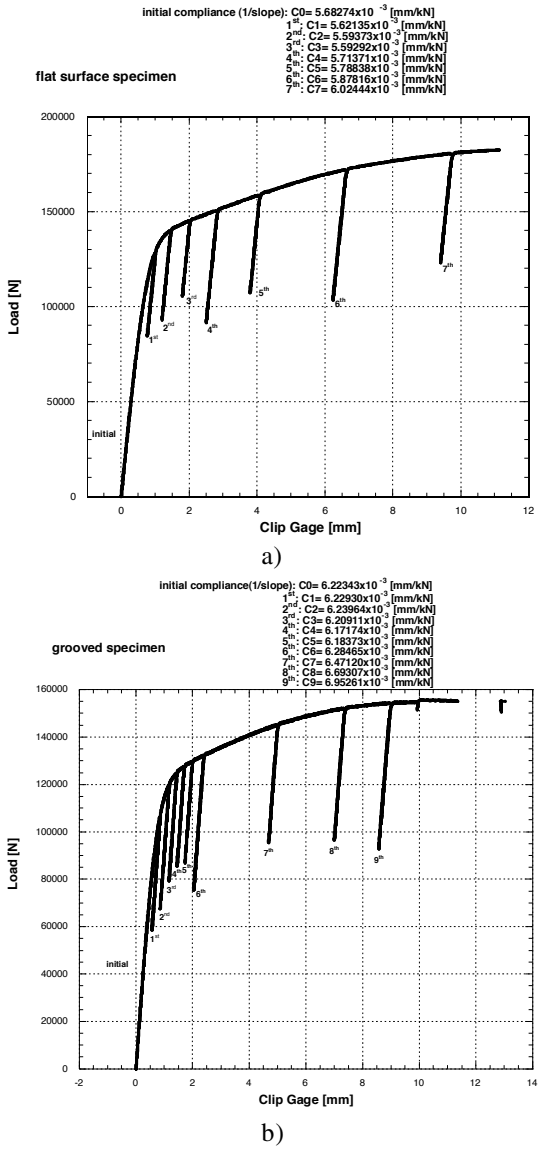

Fig. 2. Overall load versus clip gage displacement; a) flat surface; b) grooved specimen.

The result of J as a function of clip gage displacement is presented in Figure 7, displaying the typical shape these curves, see *eg* [1,2,5] for testing using multiple

specimens.

The equations of ASTM E1820 were used for data treatment. Tables A1 and A2 in Annex presents the detailed calculations performed for both specimens (flat and side grooved specimens, Table A1 and Table A2 respectively), leading to the *J* resistance curves of Figure 8.

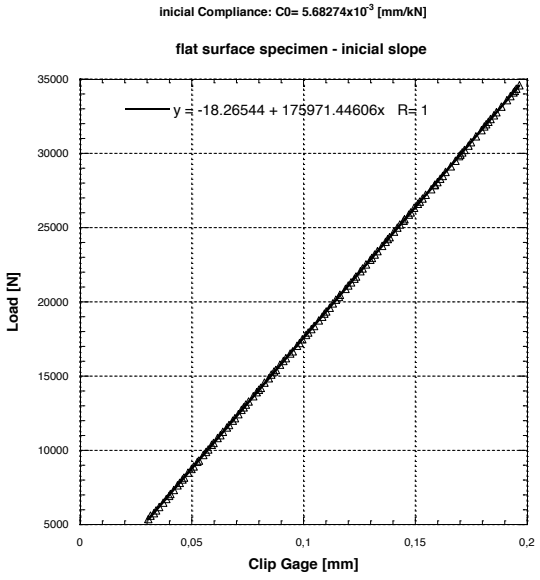

a)

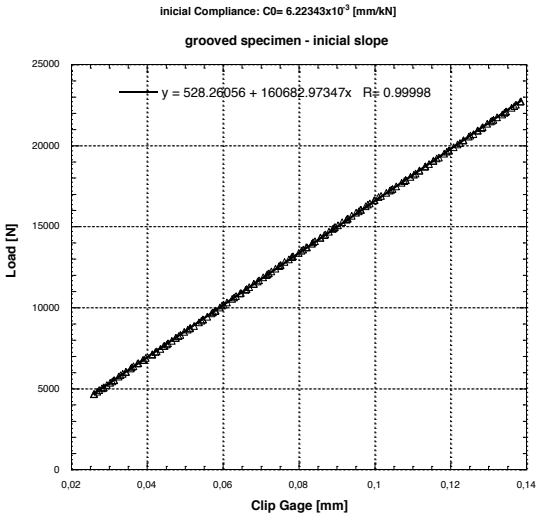

b)

Fig. 3. Detail of the load versus clip gage for the initial elastic loading of each specimen; a) flat surface; b) grooved specimen.

The rotation correction factor mentioned in [11] was not used in this work. Loss was the first to propose a compliance correction factor for the calculation of crack length from experimental compliance data, [17], still included in the current ASTM standards [11].

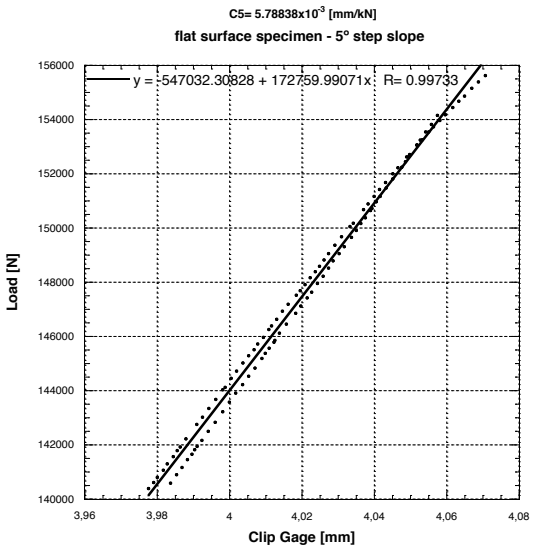

Fig. 4. Unloading compliance for 5th unloading step, for the flat surface specimen.

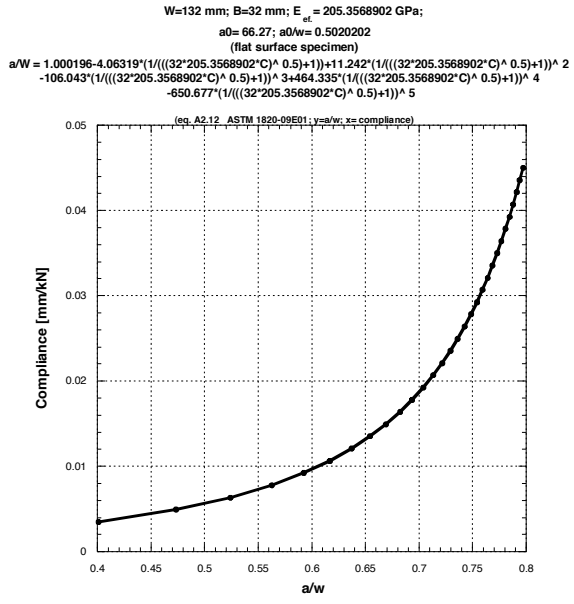

Fig. 5. Compliance calibration $C = f(a/W)$ for the flat surface specimen.

However, the legitimacy of that approach is being disputed: in the context of a revised approach based on elasto-plastic FEM modelling, Bao and Cai [18] state state that 'if one considers the rotation effect of the CT specimen on the crack length measurement, the corrected compliance formula recommended in the current test standard will lead to a larger error than that without rotation correction'. Given those circumstances, the rotation correction issue is left for

further research, and the present paper concentrates on comparing the behaviour of flat side and side grooved specimens using directly the compliance measurements performed.

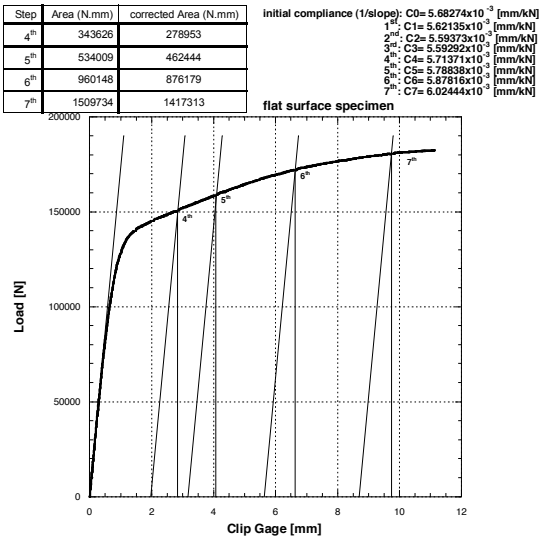

Fig. 6. Calculation of the relevant areas for performing the evaluation of J for each data point of the test (*ie*, for each unloading performed); a) flat surface; b) grooved specimen.

Finally, Figure 9 presents the simultaneous plot of the recorded load line displacement (measured using a clip gage) and of crack growth during test, as inferred from the compliance calibration and unloading compliance measurements performed.

4. Discussion

One 20% deep 90º side-grooved specimen and one flat surface specimen, both with 32mm overall thickness, were tested for fracture toughness determination. Testing consisted on monotonic loading, recording actuator displacement, load-line displacement measured using a clip gage, and load. The load-line displacement is intended for evaluation of ductile tearing using compliance measurements during partial unloadings.

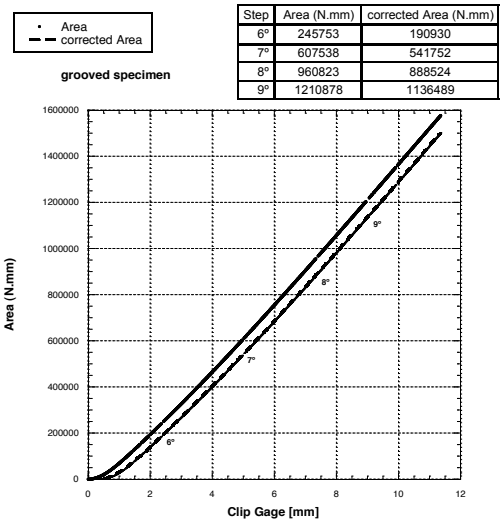

Fig. 7. J as a function of clip gage displacement, for the grooved specimen.

The unloading compliance technique was chosen to estimate stable crack growth during the tests, and accurate load line displacement measurements were performed using a clip gage. Stress intensity factor (K) and compliance calibrations as a function of crack length/width ratio, published by ASTM, were used to derive the J R-curve.

A drop in fracture toughness was observed for the grooved specimens, as expected given its higher triaxiality: the R-curve for the flat surface specimen is higher than that for the grooved specimen, and the estimated J at initiation of stable crack propagation is also slightly higher for the flat surface specimen.

For the purpose of comparison, the maximum load $J_{0,max}$ value was obtained using actuator displacement record. Although the elastic behaviour of the specimens is grossly misrepresented by actuator displacement, a reasonable agreement was obtained for the maximum load measurements. It is observed that, in the case of the present tests, while measurements of elastic behaviour require adequate

clip gages, the values of toughness associated with the test maximum load can be reasonably captured using actuator displacement, a fact due to the predominant large plastic strains at that level of load.

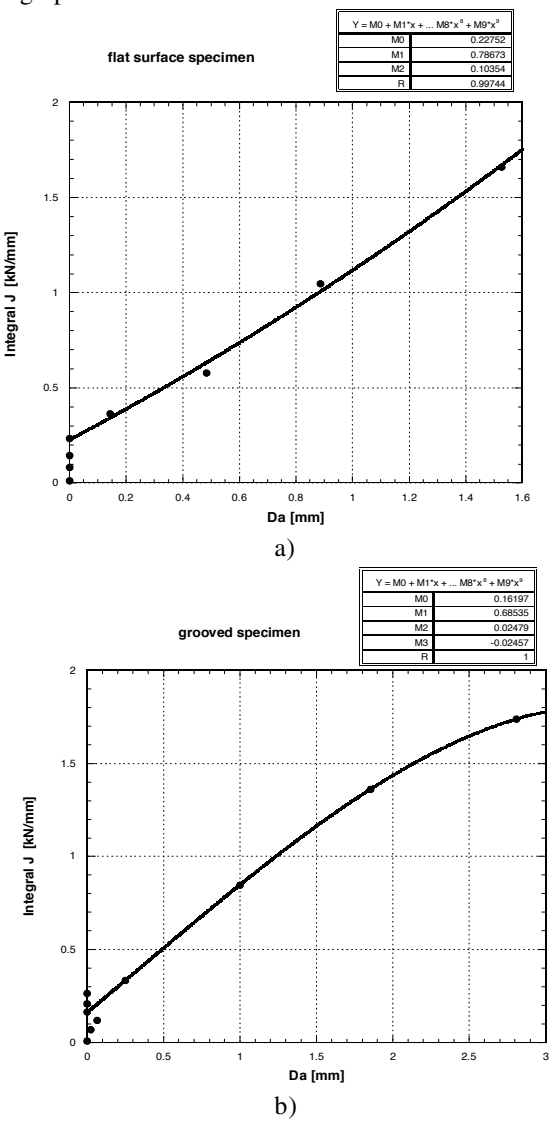

Fig. 8. *J* resistance curves; a) flat surface; b) grooved specimen.

Given the relatively high complexity of the experiments involving a clip gage on the load line, and for the sake of comparison, actuator displacement records were used for a simplified assessment of toughness considering the tests maximum load. The criteria of [13] (section 6.3.1.1, page 43), was used for the evaluation of $J_{0,max}$ and those values were taken as toughness of the present specimens, where K is calculated for the point of interest (P_{max} in this work), and J_{pl} is the plastic component of J, as presented for example in ASTM E1820, [11]. The results obtained are $J_{0,max}$=1.69 kN/mm in the case of the grooved specimen and 2.04 kN/mm in the case of the flat surface specimen, [16, 19]* .

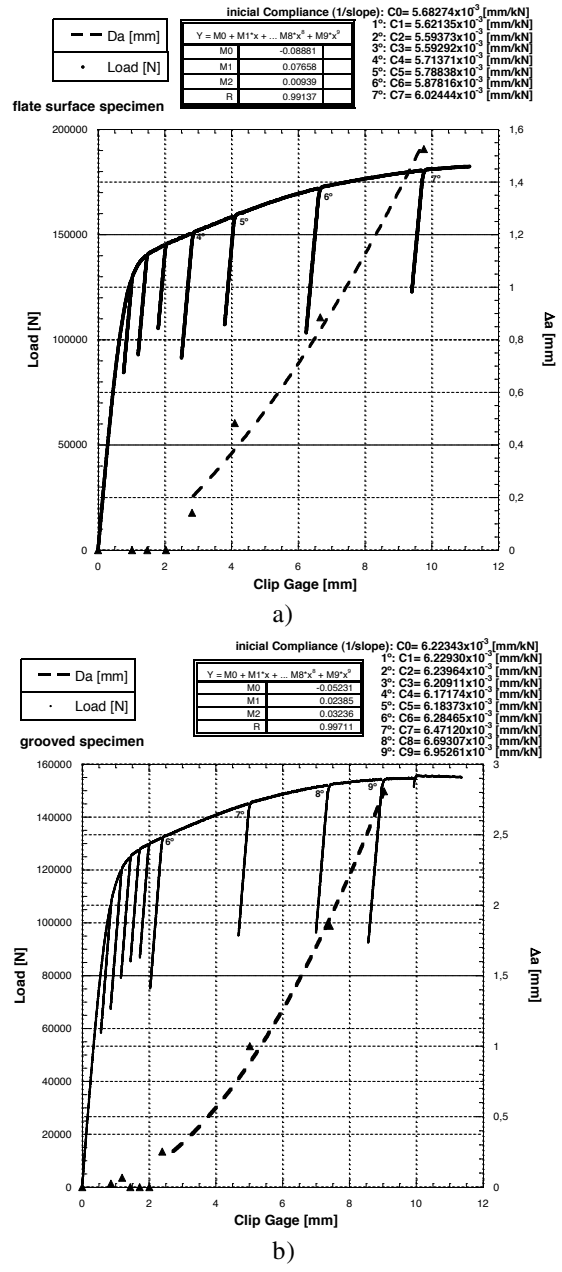

Fig. 9. Simultaneous plot of the recorded load line displacement and of crack growth during test; a) flat surface; b) grooved specimen.

* A typo was identified in those references, where by mistake the grooved specimen $J_{0,max}$ was stated as 0.38kN/mm instead of the correct 1.69 kN/mm. Further, in [19] there is a typo concerning the flat surface toughness, 0.204kN/mm instead of the correct 2.04kN/mm.

These are likely to be overestimates given use of actuator displacement in the calculations, but nevertheless agree reasonably well with the trend of the load line clip gage compliance measurements; although actuator displacement does not reflect the specimen elastic behaviour, the reasonable agreement found is attributed to the predominance of the plastic behaviour in both tests performed.

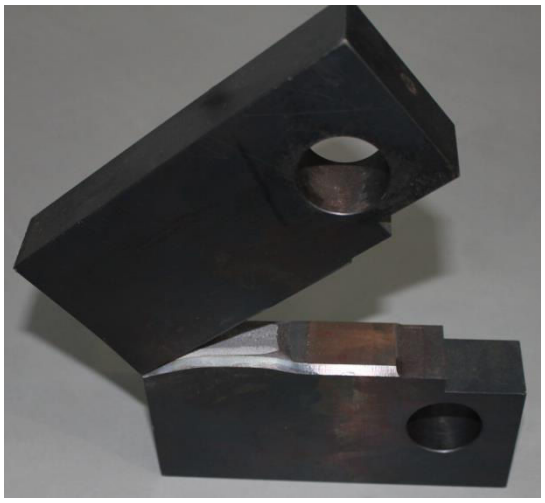

Fig. 10. Grooved specimen after testing.

Fig. 11. Flat surface specimen after testing, revealing typical plane stress behaviour.

Side-grooving increases the degree of plane strain, and therefore implies a reduction of toughness, as verified in the present experimental work.

Figure 10 shows the side-grooved specimen after testing, whereas Figure 11 shows the characteristic plane stress behaviour displayed by the flat surface specimen.

Although a discussion could be made concerning the region of Δa close to the origin, including reference to a blunting line and other aspects of that region, see eg [11], it was decided to present all the data as obtained through the data treatment method followed, as frequently found in this type of studies, see *eg* [20,21].

5. Concluding Remarks

The R curve of a structural steel was characterized using the unloading compliance technique. An effect of side grooving was found, consisting of lower R-curve and slightly lower J initiation values for the grooved specimen. Even if the actuator displacement is inappropriate for measurements of specimen strains and displacements, J at the maximum load obtained using the rigorous load line displacement and actuator displacement was approximately similar, a fact resulting of the predominant plastic behaviour of the specimens.

Acknowledgements

The steel was kindly supplied by Teixeira Duarte SA. The specimens were designed by Carlos Albuquerque for a programme of fatigue crack characterization of the steel used in the Álcacer do Sal railway bridge built for REFER, published elsewhere. The initial maximum load interpretation of the tests was done in the frame of the MSc thesis of Christoph Sebastian Thies at DEMec FEUP in 2012.

References

[1] J. A. Begley, J. D.Landes, ‘The J integral as a fracture criterion’, in: ‘Fracture Toughness’, Proceedings of the 1971 National Symposium on Fracture Mechanics, Part II, ASTM STP 514, American Society for Testing and Materials, pp.1-20, 1972

[2] J.D. Landes, J.A.Begley, ‘The effect of specimen geometry on Jic’, in: ‘Fracture Toughness’, Proceedings of the 1971 National Symposium on Fracture Mechanics, Part II, ASTM STP 514, American Society for Testing and Materials, pp. 24-39, 1972

[3] J.A. Begley, J.D. Landes, ‘Test results from J-integral studies: an attempt to establish a testing procedure’, in: Fracture Analysis, ASTM STP 560, American Society for Testing and Materials, pp. 170-186, 1974

[4] P.M.S.T. de Castro, J.C. Radon, L.E. Culver, *International Journal of Fatigue*, **1**, (3), 153 (1979)

[5] P.M.S.T. de Castro, J. Spurrier, P. Hancock, *International Journal of Fracture*, **17**, (1), 83 (1981)

[6] P.M.S.T. de Castro, *Engineering Fracture Mechanics*, **19**, (2), 341 (1984)
[7] ASTM E561 – 08, 'Standard test method for K-R curve determination', 2008, revised 2010
[8] ASTM E 399 – 08, 'Standard test method for linear-elastic plane-strain fracture toughness K_{Ic} of metallic materials', 2008
[9] ASTM E813 - 89E01, 'Test method for JIC, a measure of fracture toughness', withdrawn 1997
[10] ASTM E1737 – 96, 'Test method for J integral characterization of fracture toughness', withdrawn 1998
[11] ASTM E1820 – 09, 'Standard test method for measurement of fracture toughness', 2009
[12] BS 7448, 'Fracture mechanics fracture toughness tests', in 4 parts, various dates
[13] K.-H. Schwalbe, J. Heerens, U. Zerbst, H. Pisarski, M. Koçak, 'EFAM GTP02 - the GKSS test procedure for determining fracture behavior of materials', GKSS report 2002/24, 2002
[14] J.A. Joyce, 'Manual on elastic-plastic fracture: laboratory test procedure', ASTM Manual Series MNL 27, 1996
[15] C.M.C. Albuquerque, R.M.C. Miranda, V. Richter-Trummer, M.A.V. de Figueiredo, R. Calçada, P.M.S.T. de Castro, *International Journal of Structural Integrity*, **3**, (2), 184 (2012)
[16] C. Thies, C. Albuquerque, S.M.O. Tavares, V. Richter-Trummer, M.A.V. Figueiredo, P.M.S.T. de Castro, 'A contribution to the characterization of the mechanical behavior of S355NL structural steel', presented at the 1st International Conference of the *International Journal of Structural Integrity*, Porto, Portugal, June 25-28, 2012
[17] Loss, F.J., 'Structural integrity of water reactor pressure boundary components: Progress report ending 30 November 1977', NRL memorandum Report 3782, May 1978
[18] Bao, C.; Cai, L., *Acta Mechanica Solida Sinica*, **24**, (2), 144 (2011)
[19] C.S. Thies, 'Contribution to the characterization of the mechanical behavior of a structural steel, MSc thesis, Faculdade de Engenharia, Universidade do Porto, Portugal, March 2012
[20] K.-H. Schwalbe, J. Heerens, *Fatigue an Fracture of Engineering Materials and Structures*, **21**, 1259 (1998)
[21] M.E. Launey, D.C. Hofmann, J.-Y. Suh, H. Kozachkov, W. L. Johnson, R. O. Ritchie, *Applied Physics Letters*, **94**, 241910 (2009)

Annex

Table A1. Flat specimen

a [mm]	Δa [mm]	a/W	Compliance ASTM [mm/kN]	Load [kN]	Area [kN.mm]	Area corrected [kN.mm]
66.267	0	0.5020202	5.68274E-03	60	9.864	0
65.98	0	0.4998518	5.62135E-03	128.333	78.961	32.165
65.85	0	0.4988668	5.59373E-03	140	137.914	82.223
65.847	0	0.4988378	5.59292E-03	145	220.519	160.779
66.41	0.142	0.5031032	5.71371E-03	150.556	338.184	273.779
66.75	0.483	0.5056848	5.78838E-03	158.889	534.009	462.277
67.153	0.886	0.5087348	5.87816E-03	172.222	960.148	875.872
67.793	1.525	0.5135824	6.02444E-03	180.556	1509.734	1417.104

Table A1. Flat specimen, continuation.

$f(a/W)$	K [kN.mm$^{-3/2}$]	η_{pl}	J_{elast}	J_{plast}	J [kN/mm]
9.7194	1.5862	2.2599	0.010903	0	0.010903
9.6547	3.3701	2.2611	0.049215	0.034426	0.083641
9.6255	3.6653	2.2616	0.058217	0.087848	0.14606
9.6246	3.7959	2.2616	0.062438	0.17177	0.23421
9.7521	3.9935	2.2594	0.06911	0.29471	0.36382
9.8306	4.2485	2.258	0.078216	0.49992	0.57814
9.9247	4.6491	2.2564	0.093661	0.95241	1.0461
10.077	4.9491	2.2539	0.10614	1.5546	1.6607

Table A2. Grooved specimen.

a [mm]	*Δa* [mm]	*a/W*	Compliance ASTM [mm/kN]	Load [kN]	Area [kN.mm]	Area corrected [kN.mm]
68.67	0	0.5202273	6.22343E-03	50	7.954	0
68.694	0.024	0.5204111	6.22930E-03	107.403	52.371	16.476
68.737	0.067	0.5207342	6.23964E-03	120.221	87.613	42.639
68.611	0	0.5197781	6.20911E-03	125.083	120.698	72.013
68.455	0	0.5185997	6.17174E-03	127.735	154.805	104.034
68.505	0	0.5189788	6.18373E-03	129.945	194.541	141.998
68.922	0.252	0.5221331	6.28465E-03	132.155	245.112	190.766
69.669	0.999	0.5277991	6.47120E-03	145.414	609.983	544.185
70.524	1.854	0.5342742	6.69307E-03	152.486	966.479	894.125
71.479	2.809	0.5415094	6.95261E-03	154.696	1214.962	1140.496

Table A2. Grooved specimen, continuation.

f(a/w)	*K* [kN.mm$^{-3/2}$]	η_{pl}	J_{elast}	J_{plast}	*J* [kN/mm]
10.293	1.553	2.2504	0.010451	0	0.010451
10.299	3.3379	2.2503	0.048281	0.022527	0.070808
10.31	3.7402	2.2502	0.060619	0.058331	0.11895
10.278	3.8795	2.2507	0.065219	0.098341	0.16356
10.24	3.9468	2.2513	0.067502	0.14176	0.20926
10.252	4.02	2.2511	0.070028	0.19363	0.26365
10.357	4.13	2.2494	0.073915	0.26165	0.33557
10.549	4.6288	2.2465	0.092844	0.75436	0.8472
10.776	4.9585	2.2431	0.10654	1.2548	1.3613
11.04	5.1536	2.2393	0.11509	1.6231	1.7381